Initial Results from Radiometer and Polarimetric Radar-based Icing Algorithms Compared to in situ Data

David Serke
National Center for Atmospheric Research

Andrew L. Reehorst and Michael C. King
NASA Glenn Research Center

ABSTRACT

In early 2015, a field campaign was conducted at the NASA Glenn Research Center in Cleveland, Ohio, USA. The purpose of the campaign is to test several prototype algorithms meant to detect the location and severity of in-flight icing (or icing aloft, as opposed to ground icing) within the terminal airspace. Terminal airspace for this project is currently defined as within 25 kilometers horizontal distance of the terminal, which in this instance is Hopkins International Airport in Cleveland.

Two new and improved algorithms that utilize ground-based remote sensing instrumentation have been developed and were operated during the field campaign. The first is the 'NASA Icing Remote Sensing System', or NIRSS. The second algorithm is the 'Radar Icing Algorithm', or RadIA. In addition to these algorithms, which were derived from ground-based remote sensors, in-situ icing measurements of the profiles of supercooled liquid water (SLW) collected with vibrating wire sondes attached to weather balloons produced a comprehensive database for comparison. Key fields from the SLW-sondes include air temperature, humidity and liquid water content, cataloged by time and 3-D location.

This work gives an overview of the NIRSS and RadIA products and results are compared to in-situ SLW-sonde data from one icing case study. The location and quantity of supercooled liquid as measured by the insitu probes provide a measure of the utility of these prototype hazard-sensing algorithms.

INTRODUCTION

When subfreezing air becomes supersaturated with respect to water and ice, ice crystals begin to grow on freezing nuclei such as mineral dust, aerosols, other pollution particles or existing ice crystals by the process of diffusion [1]. In the absence of significant populations of such ice nuclei, liquid water drops begin to condense out of the air from the water vapor. In these situations, supercooled liquid water (SLW) drops can form, which can result in aircraft icing. In-flight icing occurs when an aircraft impacts with these SLW drops, which instantly freeze to the airframe. The resulting ice accretion builds up on the leading edges of the airframe's surfaces. A supercooled large drops (SLD) environment is defined as having a spectrum with a maximum drop diameter larger than 100 μm and can accrete well beyond the leading edges of the airframe where ice protection systems typically exist. Ice buildup while in flight acts to increase drag and reduce the aerodynamic lift generated by a vehicle's control surfaces. Significant ice buildup can degrade an aircraft's flight characteristics enough to be a significant safety hazard and has been recognized as a contributing factor to many crashes with resulting loss of life.

No single instrument has yet been developed which can unambiguously detect in-flight icing conditions remotely. For this reason, combinations of sensors have been under development for some time to detect in-flight icing [2,3]. This study will focus on methods to utilize two ground-based remote sensing platforms with the purpose of providing accurate and timely warnings on in-flight icing hazard. Each instrument platform or source of comparison data are described in detail in the following paragraphs.

INSTRUMENTATION AND ALGORITHMS

NIRSS

NASA and the National Center for Atmospheric Research have been developing NIRSS since 2003 (Fig. 1)[4]. The system employs a elevation and azimuth scanning multi-channel radiometer, built by Radiometrics Corporation, which passively collects incoming microwave radiation at a number of channels in the K and V-bands of the electromagnetic spectrum [5]. The K-band lies within an atmospheric water vapor resonance feature and thus variations at specific frequencies within the band are primarily caused by variations in the amount of liquid and gaseous water. The V-band is on the shoulder of an atmospheric oxygen resonance, so that progressively varying frequencies from the peak of the absorption feature yields information on the atmospheric temperature further from the radiometer (in range).

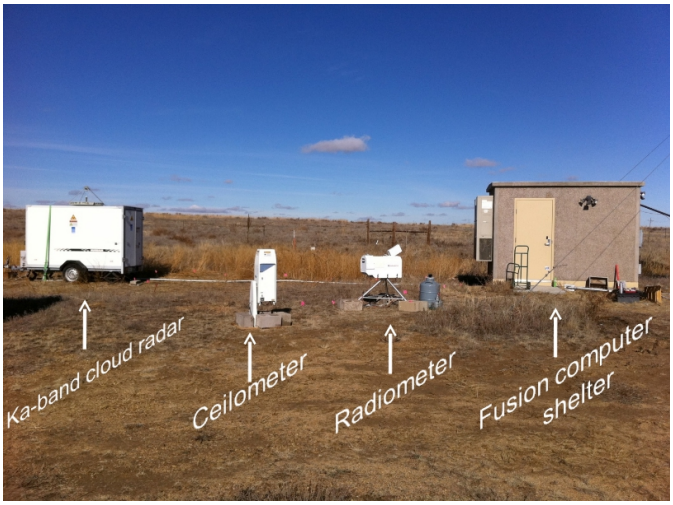

Figure 1 – Components of NIRSS, shown when they were in Platteville, CO.

Algorithms used within the radiometer's software use neural networks trained on large historical archives of integrated liquid water (ILW), integrated water vapor (IWV) and temperature profiles combined with the measured radiometric brightness temperatures to generate real-time profiles of ILW, IWV and temperature. NIRSS ingests the radiometer profiles, a Ka-band cloud radar profile built by Metek Corporation and a cloudbase height measurement from a laser ceilometer into a 'fusion' machine, then combines the instrument fields into an in-flight icing product. The height range of the 0 and -20° Celsius isotherms are targeted as the area where in-flight icing is most likely to exist from previous research flight campaigns. The vertical extent of cloud boundaries

are provided by the ceilometer and K-band cloud radar. If cloud exists within the height range where icing temperatures exist, any liquid sensed by the radiometer is then distributed vertically with fuzzy logic based on previous experience with years of research flights in icing conditions [6]. A recent study found that NIRSS detects the absence, presence and severity of in-flight icing at least as well as the FAA's current operational system for icing detection [7] in the profile viewed by NIRSS.

This technology has recently been extended to provide volumetric coverage of an airport terminal environment [8]. Building on the existing vertical pointing system, the new method for providing volumetric coverage utilizes a vertical pointing cloud radar, a multi-frequency microwave radiometer with azimuth and elevation scanning capabilities, and a NEXRAD radar. In addition to the vertical profiles provided by NIRSS, the new volumetric product adds slant-angle measurements from the radiometer to derive icing parameters along the airport's runway headings within 12.5 km of the airport center. Also, features in the NEXRAD reflectivity field are tracked with time to provide an advection vector with which to laterally move the NIRSS icing hazard profiles. Advected hazard values are then compared to predefined volumes of airspace in the approach paths for each runway heading as a final hazard product for ranges of 12.5 to 25 km from the airport center. This new terminal area icing remote sensing system can return temperature, estimates of liquid water content [6] and mean cloud drop size [9] as well as a qualitative icing hazard determination for each point in the terminal airspace.

RadIA

The national network of Doppler radars, known as NEXRADs ('NEXt-generation RADars', or WSR-88Ds), were originally designed to detect the presence of precipitation-sized particles, such as snow, rain and hail (Figure 2). These operational radars were recently upgraded to have both vertical and horizontal transmit and receive capabilities, known as 'dual-polarimetric'. Dual-polarimetric radars collect additional information that can give researchers insight as to the mean particle shape, size, phase (liquid or solid), bulk density and preferred particle orientation in a given sampled volume. Polarimetric radars collect differential reflectivity (Zdr), correlation coefficient ($_{\rho}$HV) and specific differential phase ($_{\Phi}$DP). Differential reflectivity is the ratio of horizontal co-polar received power to the vertical co-polar return. One way to interpret this field is a power-weighted mean axis ratio of the particles in the volume. Cloud drops are nearly spherical, so Zdr values are near zero and tend to have small reflectivities. Larger drops become somewhat oblate as they fall and thus have Zdr values between +0.3 and +2.0 dB. Oriented ice crystals also have Zdrs that are positive and large. $_{\rho}$HV is the correlation between horizontal and vertical co-polar received returns. Wet or tumbling particles and mixed phase conditions result in decorrelation in polarizations so that $_{\rho}$HV values are typically below 0.92. Homogeneous rain or ice result in $_{\rho}$HV values above 0.95.

Detection of SLW with particle identification algorithms [10] was previously attempted with relatively poor results [11]. This was true because the cross-sectional dimension of SLW drops are often several factors of ten smaller than the precipitation particle categories that the NEXRADS were designed to detect [12]. This means that if a radar was viewing a sample volume that contained one large snowflake and a million much smaller SLW drops, the returned power to the radar receiver would be dominated by the single large snowflake. This fact, along with knowledge that the dual-polarimetric characteristics somewhat overlap for liquid and various generalized ice crystal habits, limits the radar's capacity to directly detect SLW drops.

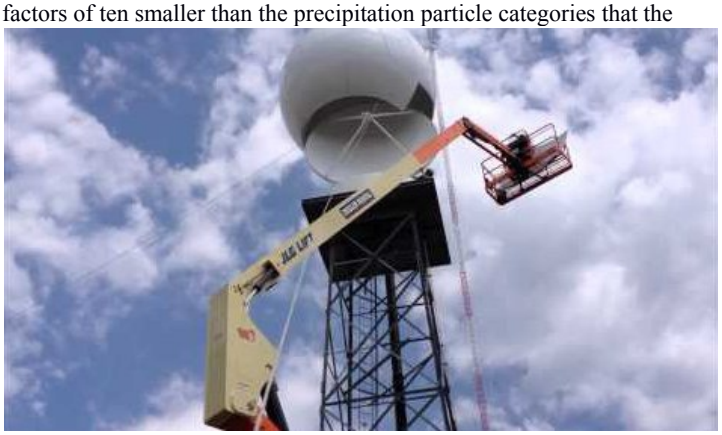

Figure 2 – NEXRAD antenna with radome

In the past several years, research flights into small drop, large drop and mixed-phase icing have shown a possible way around these seemingly insurmountable shortcomings in point-by-point radar moment analysis for icing detection. RadIA [13] uses polarimetric moment fields from operational S-band weather radars plus a temperature profile from a numerical weather prediction model as inputs. The height of the freezing level is first determined from the polarimetric moment data and then this height is used to make adjustments to the model temperature profile. Non-meteorological targets and radar return at non-freezing heights in the volume are masked out. Fuzzy logic membership functions are then defined, based on the work in the following references, to determine the presence of freezing drizzle ('FRZDRZ' algorithm in RadIA)[14], homogeneous supercooled liquid drops that are smaller than drizzle-sized ('SLW' algorithm in RadIA)[15], mixed phase conditions ('MIXPHA' algorithm in RadIA)[16] and the existence of plate-shaped crystal species ('PLATES' algorithm in RadIA)[16]. The PLATES algorithm identifies regions of crystals whose major axis dimension is much larger than their minor axis, similar to a dinner plate. These crystals, either dendrites or solid plates, tend to fall with their major axis preferentially oriented horizontally, resulting in positive Zdr values. These RadIA-specific categorical labels for particle species are referenced for the rest of this work and are not to be confused with traditional definitions for large (freezing rain, freezing drizzle) and small (cloud drop size) in-flight icing. Merging RadIA drop detection parameters to traditional definitions of microphysical particle species would require a research aircraft flight campaign, which so far has not materialized. The component weighting functions for SLW, FRZDRZ, MIXPHA and PLATES are shown in Figure 3 and range from a value of 0 for 'no icing interest'

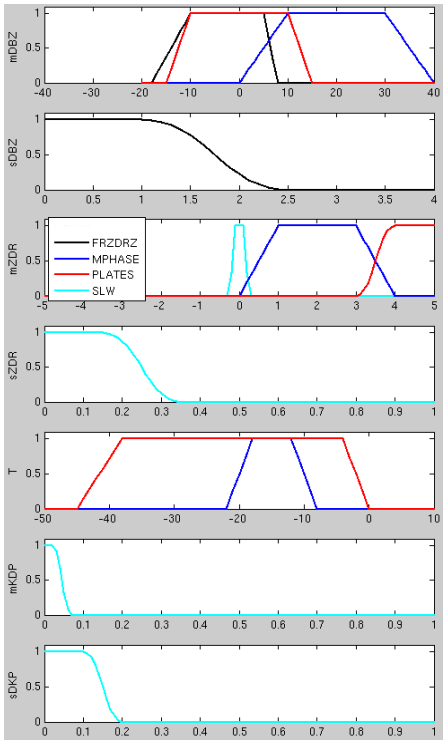

Figure 3– Polarimetric moment weighting functions for the component algorithms of RadIA

to 1 for 'maximum icing interest'. The y-axis indicates the field in capital letters (example: DBZ is reflectivity) and the prefix letter of 'm' refers to 'mean' or 's' refers to 'standard deviation'. The resulting interest values of each of these four calculations are combined through rule-based thresholding to identify areas of the radar volume that are deemed to have a high, medium or low interest in the presence of these three previously mentioned forms of in-flight icing and to define no icing interest when plate crystals are present.

SLW-sondes

A new vibrating wire sonde has been under development by Anasphere, Inc. for the past several years (Figure 4). The sondes have recently been flown in known icing conditions and compared to output from ground-based radiometers [17] as well as an in-flight icing research flight [18]. A separate presentation at this conference (no available paper) detailing recent developments with the SLW-sondes is given by Michael King from NASA Glen Research Center.

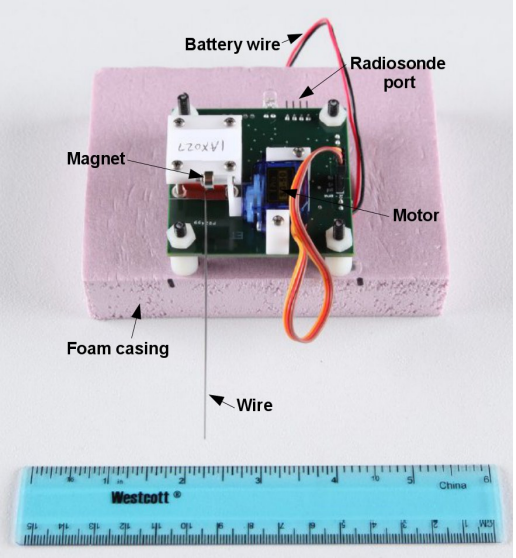

Figure 4 – SLW-sonde. Wire vibration is orthogonal to the relative airflow.

Pilot Reports

Pilot Reports (PIREPs) are voluntary reports made by commercial airline pilots of the time and location of meteorological conditions that their aircraft has encountered. In-flight icing is one of many possible conditions that can be reported. The existence of icing can be reported as 'none' or 'icing exists' as 'trace', 'light', 'moderate', 'severe' or 'heavy' severity. The authors converted these qualitative conventions to a 0-8 scale of severity for quantitative comparisons. Any icing PIREPs within 50km of Cleveland-Hopkins Airport were used as qualitative comparisons of the existence of icing for the two ground-based algorithms.

2015 WINTER FIELD CAMPAIGN

OVERVIEW

To address the goals of this study, the authors operated NIRSS and RadIA at NASA Glenn Research Facility in Cleveland, Ohio throughout the winter of 2015. Positions of the respective instrumentation for this field campaign are shown in Figure 5. The field instrumentation are within 200 meters of each other. The radiometer scan volume includes zenith and 10° elevation scans along the four runway headings at 58, 101,

Figure 5 – Location of field campaign instrumentation. The NASA hangar is 20 x 76 meters.

238 and 281° azimuth, which is repeated every 5 minutes. In the absence of expensive icing flights flown with specially outfitted research aircraft, verification and validation of the presence of in-flight icing were provided by pilot reports and by the balloon-borne SLW-sondes. PIREP times and icing severities were used only as an indicator of the presence of in-flight icing conditions within the study area.

Case Study: January 22nd, 2015

On January 22nd, 2015, a short-wave trough moved through the Cleveland area. The short wave was associated with a persistent low pressure system located over the Hudson Bay region (not shown). The local surface temperatures were -4.4 °C with dew point temperatures around -6.6 °C. Winds were around 2 ms^{-1} from the northwest, shifting to the southwest at the time of the sonde release. The local automated weather reported station was reporting light snow, fog and mist changing to light snow at the surface at the time of the sonde release. Several positive icing PIREPs were reported in the Cleveland terminal airspace from 13:14 to 15:15 UTC on this date, including two 'moderate' icing severities. The PIREPs around the time of the sonde indicated icing between 670 and 2100 m AGL. A SLW-sonde was released from the NASA Glen Reseach Center grounds at 14:17 UTC. The thermodynamic profile (Figure 6, part A) shows a vertically complex cloud that is formed from multiple layers merging to create one continuous cloud from 0.2 to 2.3 km above ground level (AGL), with temperatures in the prime icing range of -6° C near cloud base to -12°C at cloud top. The vibrational frequency of the wire (part B) is seen to start decreasing from a starting value near 44.5 Hz as it gets into the cloud layer and levels out near cloud top at a value near 43.5 Hz. The total decrease in frequency through the cloud layer was approximately 1 Hz. LWC results are estimated from the change in frequency per unit height per unit time [17] and the derived profile is shown in Figure 6, part C. Temperature inversions in a saturated environment at 0.8 and 1.4 km AGL (black horizontal lines) are colocated with relative or absolute maximums in SLW-sonde LWC. The temperature inversion at 2.3 km corresponds with the height of cloud top and SLW-sonde LWC extinction. The presence of these temperature inversions within the cloud layer, even very small ones, indicate the presence of atmospheric lifting and subsequent saturation of discrete layers within the cloud depth. Maximum LWC of 0.35 gm^{-3} occurs at 0.8 km AGL and then rapidly reduces to near zero at 1 km AGL. The top half of the cloud has a relative maximum of 0.15 gm^{-3} just above 1.2 km AGL before the LWC gradually is reduced back to zero by the cloud top height of 2.3 km.

Reflectivity (Figure 7) and differential reflectivity (Figure 8) plots from the polarimetric Cleveland NEXRAD at the 3.5 degree elevation 'tilt' are shown, as they are key ingredients to RadIA. Only weak reflectivities in the range of -20 to 0 dBZ are evident, with

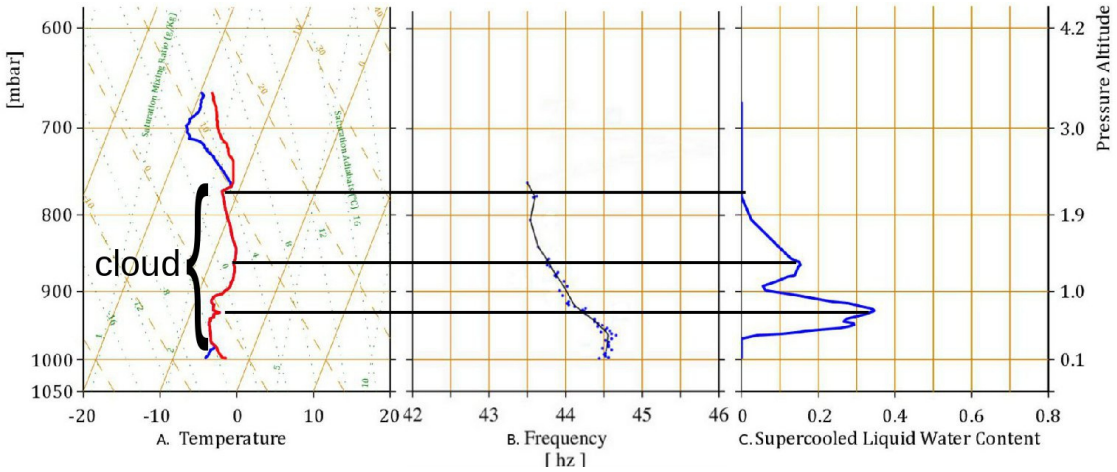

Figure 6 – Profiles of temperature (red, A) and dewpoint temperature (blue, A), sonde wire frequency (blue dots, B) and LWC (C) for the balloon launch at 14:17 UTC on January 22nd, 2015.

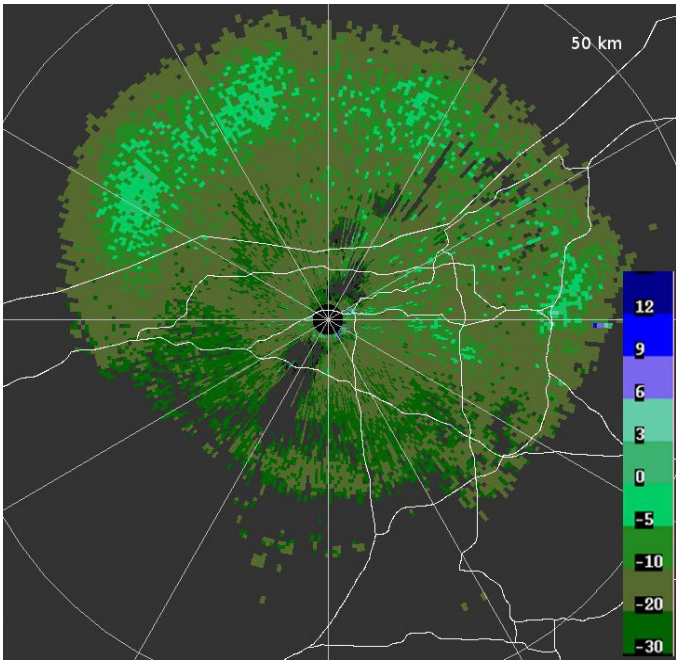

Figure 7 – 3.5º elevation NEXRAD tilt reflectivity[dBZ] at 14:01 UTC on January 22nd, 2015.

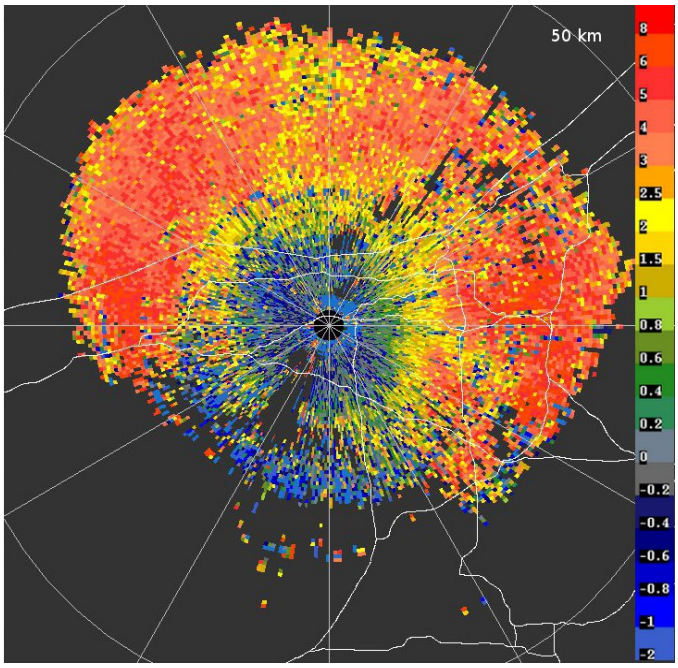

Figure 8 – 3.5º elevation NEXRAD tilt Zdr [dB] at 14:01 UTC on January 22nd, 2015.

detectable returns terminating at around 37 km range at this tilt angle. This range corresponds to the highest precipitation sized particles existing up to about 2.1 km AGL. The corresponding Zdr plot has very high values in the top half of the cloud, on the order of +4 to +7 dB, which indicates the presence of highly oriented, axially asymmetric crystals. Near zero to slightly negative Zdr values in the lower third of the cloud indicate the dominance of round particles.

RadIA output is shown in Figure 9. The colorbar shows where positive icing is identified by specific algorithms within RadIA. The salmon color is icing due to drops smaller than drizzle (RadIA's 'SLW'), brown is freezing drizzle and larger (RadIA's 'FRZDRZ', abbreviated 'FRZ'), yellow is both SLW and FRZDRZ, white are plate-shaped crystals (RadIA's 'PLATES'), dark grey is when all algorithms show no icing and light grey is when RadIA has no classification. Horizontal range rings were added to the figure, within which certain RadIA icing hazard classifications are seen to dominate. SLW is prevalent within about 10 km range of the radar, FRZDRZ dominates from 10 to 18 km range and patches of FRZDRZ separated by areas of PLATES from 18 to 37 km range. The development through time of the spatially continuous regions of plate-shaped crystals in RadIA's PLATES algorithm is likely due to the rapid growth of needles, dendritic or hexagonal crystals, as discussed in reference 16. Dendrites grow in water saturated environments at the expense of the supercooled liquid detected near the top of the cloud by RadIA's FRZDRZ algorithm. The overall hazard output of RadIA is somewhat speckled in nature due to the removal of ground clutter pixels by the particle identification algorithm in an earlier processing step. No smoothing of any kind has been done on the RadIA output.

The heights of the dominant algorithm-detected icing conditions, as defined by RadIA and delineated by the rings in Figure 9, are plotted in a vertical format on the right side of Figure 10. Icing detected by RadIA's cloud-sized SLW drop algorithm dominates from the surface up to roughly the height of the maximum SLW-sonde LWC value at 0.8 km AGL. Above that, freezing drizzle dominates up to around 1.1 km, where sonde LWC values drop significantly back toward zero. Above 1.1 km AGL, sonde LWC reaches a relative maximum before eroding away significantly with height as the cloud top is approached. In this portion of the cloud, freezing drizzle pockets still exist in RadIA, but large, continuous areas dominated by plate-shaped crystals are interspersed. Perhaps the crystals are

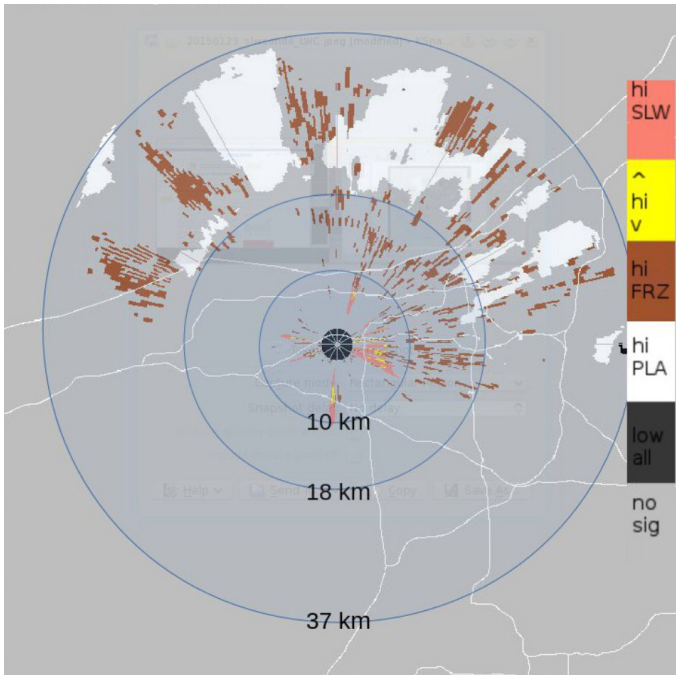

Figure 9 – 3.5° elevation tilt RadIA classification of the NEXRAD moments at 14:01 UTC on January 22nd, 2015.

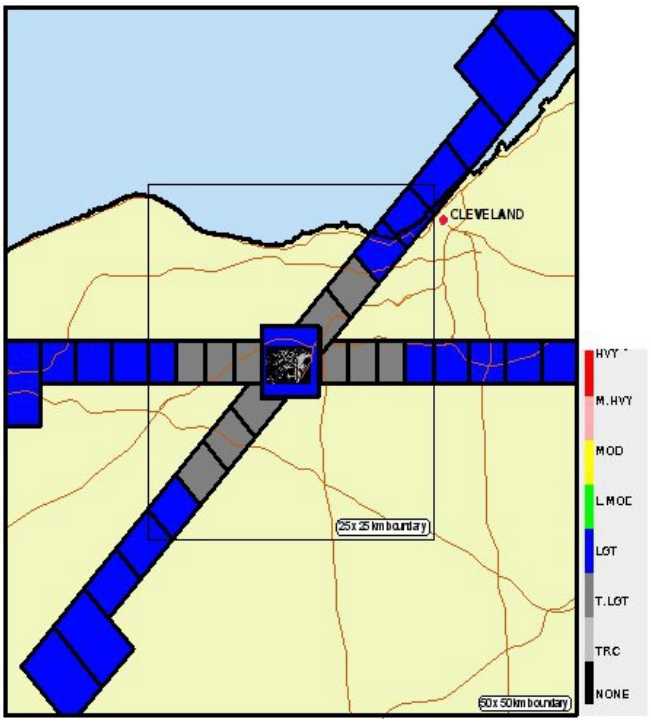

Figure 11– NIRSS volumetric product at 14:15 UTC on January 22nd, 2015.

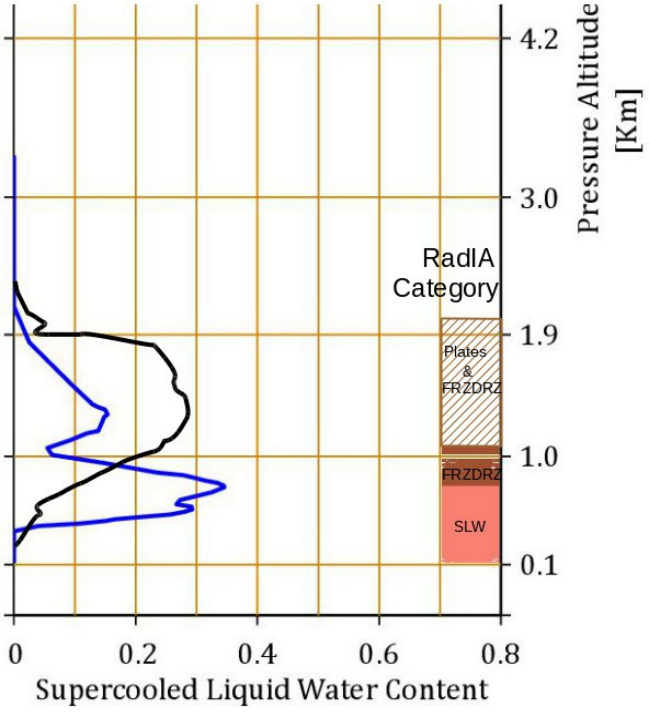

Figure 10 – SLW sonde (blue) and NIRSS (black) LWC [gm^{-3}] with RadIA classification profile.

responsible for the erosion of the LWC values as one approaches the upper levels of the cloud. Ice crystal growth scavenging existing SLW is a commonly observed and well understood path to the erosion of in-flight icing conditions.

The derived LWC 'profile' from the sonde (blue line) and the derived LWC profile from the colocated NIRSS platform (black line) are also shown on Figure 10. It is important to note that the collection efficiency of the SLW-sonde's vibrating wire, and thus the derived LWC profile, depends on drop size [17]. The sonde values are not really from a vertical profile, rather they are a slant path defined by the ascent rate and horizontal winds experienced by the balloon. The NIRSS LWC profile is computed by distributing the radiometer-sensed integrated liquid through the depth of the Ka-band sensed cloud layer through a fuzzy-logic algorithm that relies on idealized relationships between temperature, reflectivity and the assumption of wedge-shaped profiles. Significant differences exist in these two estimated LWC profiles, such as the height of the absolute maximum in LWC. This is due to NIRSS having a more wedge-shaped output due to the dominant weighting of an idealized wedge-shaped profile in the NIRSS logic. The overall magnitude and height bounds of the NIRSS-derived LWC is comparable to that derived from the sonde. Differences in these two LWC products can be partially attributed to the radiometer channels sampling 4-6° angle viewing cones [5] whereas the sondes are essentially time-varying point measurements.

The terminal area NIRSS product, shown in Figure 11, is the result of a recent development effort to extend the ground-based remote sensing aviation hazard detection to the runway approach vectors. In this plot, the maximum NIRSS hazard values within the range-segmented, FAA-defined glide paths for commercial aircraft operating in the Cleveland airspace are color-coded for 'none', 'trace', 'light', 'light/moderate', 'moderate', 'moderate/heavy' and 'heavy' icing severity categories. The box which includes the immediate terminal area is assigned the maximum hazard level given in the profile as determined by the vertically pointing NIRSS (In this case 'light' severity, colored blue). The hazard value for the four boxes along each runway heading within 12.5 km (6.7 nautical miles) of the terminal are assigned the maximum NIRSS hazard within each box volume defined by the 10 degree slant angle radiometer ILW distributed over the given vertical cloud profile. Finally, the hazard value for boxes along each runway heading between 12.5 and 25 km (6.7 and 13.5 nautical miles) are defined by maximum NIRSS hazard within each box volume as defined by the closest slant angle NIRSS hazard profile as advected by radar detected features. This is the first case that the terminal area NIRSS product has been applied to, and

the magnitude of the resulting icing in each approach volume seems at least reasonable given the SLW-sonde results that have been discussed in previous figures.

SUMMARY

During this past winter, an in-flight icing hazard detection field campaign was conducted in Cleveland, Ohio, USA where output from two ground-based remote sensing platforms/algorithms were compared to SLW profiles collected from vibrating wire sondes attached to weather balloons. This work explores the results from one case study conducted on January 22nd, 2015 which had several in-flight icing reports by commercial pilots. The polarimetric radar-based RadIA detected SLW from cloudbase up to the height at which the SLW-sonde detected a maximum LWC of 0.35 gm^{-3}. Above the maximum liquid height, RadIA detected freezing drizzle/SLD. In the top half of the cloud layer, LWC appeared to erode away toward zero with height. RadIA suggests a possible cause of that is an increase with time of preferentially-oriented plate-shaped crystals, either dendrites, hexagonal crystals or needles, which are known to grow at the expense of supercooled liquid. This high Zdr 'brightband' , which in this case is not associated with a freezing level, From this and other cases collected during the January to April of 2015 period (not shown here, see https://wiki.ucar.edu/display/TAIWIN/), RadIA has shown skill in identifying the location of icing within NEXRAD radar echo through texture and absolute values of the areally averaged polarimetric moments when compared to SLW-sonde flights.

The NIRSS-derived LWC profile was wedge-shaped with a maximum in the upper half of the cloud, but the overall magnitude of the LWC maximum and ILW was quite comparable to the SLW-sonde. When the significant differences with which LWC was measured are considered, the differences in shape and magnitude of LWC from NIRSS seem quite reasonable. A first look at an airport terminal area NIRSS product was provided and discussed. The new product provides a two-dimensional output of a three-dimensional product for range-segmented airspace volumes centered along FAA mandated runway approach vectors. The product gave reasonable qualitative 'light' icing severity values for this case, considering that the segmented approach airspace volumes (shown 2-dimensionally in Figure 11) were all within the lowest 1 km AGL of the NIRSS LWC profile (Figure 10).

Future work includes the archiving, quality control and analysis for all field campaign datasets that were collected during the January to March of 2015 case study period. An extensive analysis catalog should be available by early 2016. Comparison to numerical weather prediction model output will also be conducted as part of the overall final analysis.

REFERENCES

1. Rogers, R., and Yau, M., "A Short Course in Cloud Physics", Elsevier Science, Oxford, UK, 1988.

2. Politovich, M.K., B.B. Stankov and B.E. Martner, "Determination of liquid water altitudes using combined remote sensors", *J. Appl. Meteor*., **34**, pp. 2060—2075, 1995.

3. Bernstein, B., McDonough, F., Politovich, M., Brown, B., Ratvasky, T., Miller, D., Wolff, C., and Cunning, G., "Current Icing Potential: algorithm description and comparison to aircraft observations", *J. Appl. Meteor*., **44**, pp. 969-986, 2005.

4. Reehorst, A.L., Brinker, D.J., Ratvasky, T.P., "NASA Icing Remote Sensing System: comparisons from AIRS–II," NASA/TM—2005-213592, 2005.

5. Solheim, F., Godwin, J., Westwater, E., Han, Y., Keihm, S., Marsh, K., and Ware, R., "Radiometric profiling of temperature, water vapor and cloud liquid water using various inversion methods", *Radio Sci.*, **33**, pp. 393-404, 1998.

6. Reehorst, A., Politovich, M., Zednik, S., Isaac, G. and Cober, S., "Progress in the development of practical remote detection of icing conditions", *NASA/TM 2006-214242*, NASA, 2006.

7. Johnston, C., Serke, D., Adriaansen, D., Reehorst, A., Politovich, M.,Wolff, C. and McDonough, F., "Comparison of in-situ, model and ground based in-flight icing severity", *AMS Conference Preprint*, Seattle, WA, Jan 24-27, 2011.

8. Reehorst, A. and Serke, D., "A Terminal Area Icing Remote Sensing System", Report NASA/TM 2014-218417, 2014.

9. Serke, D., Reehorst, A., and Politovich, M. K., "Supercooled large drop detection with NASA's Icing Remote Sensing System", SPIE Remote Sensing Preprint, Sept. 19-22, Toulouse, FR, 2010. [DOI:10.1117/12.863176].

10. Vivekanandan, J., Zrnic, D., Ellis, S., Oye, R., Ryzhkov, A. and Straka, J., "Cloud microphysics retrieval sing S-band dual-polarization radar measurements", *Bulletin of the American Meteor. Soc*., **80**, 381-388, 1999.

11. Kimberly L. Elmore, 2011: The NSSL Hydrometeor Classification Algorithm in Winter Surface Precipitation: Evaluation and Future Development. *Wea. Forecasting*, **26**, 756–765. [doi: 10.1175/WAF-D-10-05011.1]

12. Bringi, V. and Chandrasekar, V., "Polarimetric Doppler Weather Radar – Principles and applications.", *Cambridge University Press*, 656 pp., 2001.

13. Serke, D., Scott Ellis, John Hubbert, David Albo, Christopher Johnston, Charlie Coy, Dan Adriaanson and Marcia Politovich, In-flight icing hazard detection with dual and single-polarimetric moments from operational NEXRADs, AMS Radar, September 16-20, Breckinridge, CO, 2013.

14. Ikeda, K., Rasmussen, R., Brandes, E. and McDonough, F., "Freezing Drizzle Detection with WSR-88D Radars", *J. Appl. Meteor. Climatol.*, **48**, 41–60, 2009. [doi: 10.1175/2008JAMC1939.1]

15. Plummer, D., Göke, S., Rauber, R. and Di Girolamo, L.,"Discrimination of mixed- versus ice-phase clouds using dual-polarization radar with application to detection of aircraft icing regions", *J. of Appl. Meteor. and Clim.*, **49**, Issue 5, pp. 920-936, 2010. [doi: 10.1175/2009JAMC2267.1]

16. Williams, E., D. Smalley, M. Donovan, R. Hallowell, K. Hood, B. Bennett, R.Evaristo, A. Stepanek, T. Bals-Elsholz, J. Cobb, J. Ritzman, A. Korolev, and M.Wolde, 2014: Measurements of Differential Reflectivity in Snowstorms and Warm Season Stratiform Systems. J. Appl. Meteor. Climatol. [doi:10.1175/JAMC-D-14-0020.1], in press.

17. Serke, D., Hall, E., Bognar, J., Jordan, A., Abdo, S., Seitel, K., Nelson, M., Ware, R., McDonough, F. and Marcia Politovich, "Supercooled liquid water content profiling case studies with a new vibrating wire sonde compared to a ground-based microwave radiometer", Atmospheric Research, June 6th, 2014. [DOI: 10.1016/j.atmosres.2014.05.026]

18. Serke, D., Doyle, R., King, M., Geerts, B., Steiger, S. and

Politovich, M., A new SLW-sonde compared to research aircraft flights, AMS 17th Symposium on Meteorological Observation and Instrumentation, June 9-13, Westminster, CO, 2014.

CONTACT INFORMATION

David Serke, serke@ucar.edu, (303)-497-8311, 3450 Mitchell Lane, Boulder, CO, 80301

ACKNOWLEDGMENTS

This work was done under the NASA Transformative Aeronautics Concepts Program and the NASA Aviation Safety Research Program. The National Center for Atmospheric Research is sponsored by the National Science Foundation. Any opinions, findings and conclusions or recommendations expressed in this publication are those of the author(s) and do not necessarily reflect views of the National Science Foundation.

DEFINITIONS/ABBREVIATIONS

FAA	- Federal Aviation Administration
FRZDRZ	- RadIA's algorithm for detecting at least as large as freezing drizzle
ILW	- integrated liquid water
MIXPHA	- RadIA's algorithm for detection of mixed-phase
NASA	- National Aeronautical and Space Administration
NCAR	- National Center for Atmospheric Research
NEXRAD	- Next-Generation Radar, or WSR-88d radar
NIRSS	- NASA Icing Remote Sensing System
NSF	- National Science Foundation
PLATES	- RadIA's plate-shaped crystal detection algorithm
PIREP	- Pilot report
RadIA	- Radar Icing Algorithm
REFL	- Reflectivity
ρ_{HV}	- cross-polar correlation coefficient
SLD	- supercooled large drops
SLW	- generally Supercooled Liquid Water, also RadIA's algorithm for detection of drops smaller than freezing drizzle
Zdr	- differential reflectivity